CoV2-ID, a MIQE-compliant sub-20-minute 5-plex RT-PCR assay targeting SARS-CoV-2 for the diagnosis of COVID-19

Stephen Bustin (stephen.bustin@aru.ac.uk)
Anglia Ruskin University https://orcid.org/0000-0003-1870-6098
Amy Coward
Mid and South Essex NHS Foundation Trust
Garry Sadler
Mid and South Essex NHS Foundation Trust
Louise Teare
Mid and South Essex NHS Foundation Trust
Tania Nolan
The GeneTeam

Article

Keywords: coronavirus, pandemic, COVID-19, reverse transcription, qPCR, ddPCR

Posted Date: September 11th, 2020

DOI: https://doi.org/10.21203/rs.3.rs-75000/v1

Abstract

Accurate, reliable and rapid detection of SARS-CoV-2 is essential not only for correct diagnosis of individual disease but also for the development of a rational strategy aimed at lifting confinement restrictions and preparing for possible recurrent waves of viral infections. We have used the MIQE guidelines to develop two versions of a unique fiveplex RT-qPCR test, termed CoV2-ID, that allows the detection of three viral target genes, a human internal control for confirming the presence of human cells in a sample and a control artificial RNA for quality assessment and potential quantification. Viral targets can be detected either separately with separate fluorophores or jointly using the same fluorophore, thus increasing the test's reliability and sensitivity. It is robust, can consistently detect two copies of viral RNA, with a limit of detection of a single copy and can be completed in around 15 minutes. It was 100% sensitive and 100% specific when tested on 23 RNA samples extracted from COVID-19 positive patients and five COVID-19 negative patients. We also propose using multiple cycle fluorescence detection, rather than real-time PCR to reduce significantly the time taken to complete the assay as well as assuage the misunderstandings underlying the use of quantification cycles (Cq). Finally, we have designed an assay for the detection of the D614G mutation and show that all of the samples isolated in the Chelmsford, Essex area between mid-April and June 2020, have the mutant genotype whereas a sample originating in Australia was infected with the wild type genotype.

Introduction

The emergence of severe acute respiratory syndrome coronavirus 2 (SARS-CoV-2) in 2019 as the causal agent of the COVID-19 disease (1, 2), and the ongoing pandemic has highlighted many of the inadequacies inherent in current diagnostic testing regimens (3). As a result, the development of nucleic acid-based tests using different molecular approaches has been rapid. SARS-CoV-2 is currently identified using either PCR (4), isothermal methodologies (5, 6) or CRISPR (7, 8). Isothermal approaches typically require more development and optimisation but have the advantage of speed and are more readily implemented into point-of-care systems (9). PCR based assays have the advantage of simplicity of design, easier multiplexing potential and in most cases, greater sensitivity. Current assays using RT-qPCR, are broadly comparable, although their reported sensitivity of 500 viral copies per reaction (10) is significantly lower than generally achievable using this technology, and assays differ significantly in the speed of their overall workflow (9). Although a more recent publication describes a streamlined assay with a detection limit of 15 copies, this is based on experiments performed by spiking total human RNA with in vitro synthesised viral transcripts, and the total workflow time remains at 2 hours (11). Most SARS-CoV-2 real time PCR assays target two viral genes using real-time fluorescence-based detection methods, most commonly through the hydrolysis of a dual-labelled probe (12). Targeting more than one viral gene is important as there is a significant false negative rate for SARS-CoV-2 RT-PCR testing (13, 14). A potential challenge for any nucleic-acid based testing methods is the potential of the virus to mutate and an analysis of primer binding sites targeted by RT-qPCR assays has indeed shown that a high percentage are mutated in at least one genome (15). A mutation in a reverse primer has been shown to

affect the sensitivity of RT-qPCR assay in use early in the pandemic (10) and further mutations could lead to the occurrence of false negative results, particularly if the mutation occurs at the extreme 3' end of the primers. Since false negative results could also be due to sampling difficulties, poor recovery of RNA, the presence of PCR inhibitors or human error, it is important that the RT-qPCR assay itself is the least likely cause and includes controls to reveal as many areas of assay vulnerability as possible. Typical commercial tests use a one tube combined reverse transcription and amplification protocol, are carried out in fairly large volumes and use slow protocols with real time data acquisition that result in typical assay times of 1-1.5 hours.

The principal aim of current SARS-CoV-2 diagnostic tests is to detect unambiguously the presence or absence of viral targets. Where viral load is not being determined, there is no requirement to measure viral load and therefore, no need to run assays in real-time (16). Instead, measuring fluorescence at the beginning of the run and then again at the end, is sufficient to detect any target-dependent amplification, whilst at the same time saving the considerable time it takes to scan a plate at the end of each cycle.

Consequently, we set out to design an RT-qPCR test that can be used qualitatively or quantitatively, in addition to being sensitive, specific and fast. The Minimum Information for Publication of Quantitative Real-Time PCR Experiments (MIQE) guidelines (17) were used as the basis for establishment of the workflow, resulting in CoV2-ID, a SARS-CoV-2-specific fiveplex RT-PCR test (Figure 1). This assay ensures specificity by initially targeting multiple SARS-CoV-2 genes (Nsp10, Nsp12 and N) in line with the WHO guidelines for the reliability of results, which require at least two genomic targets for diagnostic tests (18), with neither primers and probes amplifying or detecting any other coronaviruses. The assay also includes a human control target to confirm the presence of human cells and an extraction and inhibition control artificial sequence (EICAS) that can be used to monitor the performance of the assay and detect sample-induced reaction inhibition (19). We have used droplet (dd) PCR to delineate quantification and detection limits of this assay, which can detect a single viral genomic target. Furthermore, having previously demonstrated that PCR reaction times can be significantly reduced by using shorter denaturation and polymerisation times and altering the denaturation and polymerisation temperatures (20), we have developed a high- speed qPCR protocol that can be completed in around 15 minutes, depending on the instrument used. In addition, we demonstrate the feasibility of using a multiple cycle fluorescence detection protocol to reduce assay times even further.

Materials And Methods

The details of all reagents, plastic ware and instruments are listed in the supplementary data file, Tab 1.

Sample collection, RNA extraction, selection and storage

Nasopharyngeal/nose and throat/throat samples were collected for routine SARS-CoV-2 testing by trained staff at Mid and South Essex NHS Foundation Trust Broomfield using a variety of swab types (supplementary data file, Tab 1). RNA was extracted within 24hrs of sample collection and eluted in a final volume of 50µL RNase-free water (supplementary data file, Tab 1). The standard protocol was

modified to include an incubation at room temperature for 10 minutes in a Class 1 safety cabinet, before incubating at 56ºC for 10 minutes.

All RNA samples were stored at -80ºC. Further validation of RNA sample quality was not possible due to diagnostic requirements, however subsequent testing with the EICAS assay (detailed below) provided a measure of inhibitory contamination (19).

A total of 23 clinical RNA samples, in four batches (labelled A through D), testing positive for SARS-CoV-2 and one set of five samples testing negative at Broomfield Hospital were selected at random from those remaining after routine clinical tests. 5µL aliquots were transported on ice for 3 miles from the hospital pathology laboratory to the Molecular Biology research laboratory (Anglia Ruskin University, UK). One of these samples had very high concentrations of viral RNA (A4) and so was diluted 1:100 with sterile RNase-free water and used for assay development. Eight further samples (A1 and C1-C7) were diluted 1:30 and used for optimisation, validation and comparative analyses. All samples were stored at -80ºC until further use. Two control samples were included for development of the genotyping assay (kindly donated by J. Curry, LGC, UK). This first was RNA isolated from cell culture infected with Sars-CoV-2 which was isolated from a clinical sample at Westmead Hospital (New South Wales, Australia; COVID19 was confirmed using N1/N2 and E gene RT-qPCR) and the second, a synthetic control RNA (Twist Biosciences), which were included as wild type controls for D614G genotyping.

Primers and probes

Human SARS-CoV-2 (NC_045512.2) and SARS-CoV-1 (NC_004718.3) reference sequences and a Bat SARS-like coronavirus genome (MG772933) were downloaded to the Allele ID 7 qPCR assay design software package (Supplementary data file, Tab 1) and SARS-CoV-2 specific primers and probes were designed with manual adjustments aimed at maximising the analytical sensitivity of the assay. Three SARS-CoV-2 targets, Nsp10, N-gene and Nsp12, were chosen to accommodate sequence variabilities in primer or probe locations and minimise the likelihood of a 3'-mutation at primer binding sites reducing the reliability of the assay. *JUN* was chosen as a human extraction control to verify that human nucleic acid was present in the sample; it is intron-less, has low tissue-specificity and is highly expressed in proximal digestive tract (https://www.proteinatlas.org/ENSG00000177606-JUN/tissue). The specificity of primers, probes and amplicons was analysed *in silico* using Primer-BLAST (https://www.ncbi.nlm.nih.gov/tools/primer-blast/) and BLAST (https://blast.ncbi.nlm.nih.gov/Blast.cgi).

In addition, the human SARS-CoV-2 (NC_045512.2) genomic sequence was imported to the Beacon Designer 8.2 qPCR assay design software package (Supplementary data file, Tab 1) and an LNA-based genotyping assay for discriminating the D614G mutation (A to G) was designed. Finally, two extraction and inhibition control artificial sequences (EICAS1 and 2) were designed so that they contained no matching sequences in published databases. EICAS1 is amplified using a bespoke primer set, whereas EICAS 2 was designed with terminal 5' and 3' sequences amplified by the *JUN* primers, to avoid primer interference during the multiplex PCR. EICAS1 and EICAS2 are detected by the same probe.

Upon receipt, all DNA oligonucleotides were resuspended in sterile RNase-free water at 100µMol and stored in aliquots at -20°C. The RNA oligonucleotides were diluted to $1x10^{-9}$ relative to the original stock with sterile RNase-free water and stored at -80ºC.

RT, qPCR and digital PCR

RNA extracted from clinical samples at a dedicated COVID-19 testing facility at the Broomfield Hospital Microbiology laboratory was tested for Sars-CoV-2 using a combined RT and qPCR protocol (Viasure, Supplementary data file, Tab 1). RNA (5µL neat sample) was tested in a final reaction volume of 20µL, with a protocol of 15 minute/45ºC RT step, 2-minute polymerase activation and 45 cycles of 10 seconds/95ºC denaturation and 50 seconds/60ºC annealing and polymerisation using Biomolecular Systems Mic qPCR cyclers with manual threshold setting. Clinical laboratory testing protocols regarded samples as positive for Sars-CoV-2 if a Cq<38 was recorded for either both ORF1ab and N gene targets or ORF1ab alone. The newly designed Sars-CoV-2 test described in this report, termed CoV2-ID, was validated on the 23 clinical samples (batches A-D) samples using a modified single tube RT-qPCR protocol (PrimeScript III, Takara and 1Step Go, PCRBio) with 1µL RNA in a final reaction volume of 5µL, a 5 min/50ºC RT step, 1 min polymerase activation and 40 cycles of 1 second/95°C denaturation and 1 second/60°C annealing and polymerisation. Absence of contamination was determined by running no template (NTC) and no RT (NRC) controls.

Subsequent one-step combined RT and qPCR reactions were carried out with 0.5µL RNA, of sample-dependent, varying and unknown concentration, per 5µL reaction. Where two tube reactions were carried out, 1µL RNA was reverse transcribed in 10µL with Superscript IV Vilo (Supplementary data, Tab 1) using random primers; EICAS cDNA synthesis was supplemented with specific reverse primer (R) at 10nM final concentration. RT conditions were 5 minutes at 25ºC, 5 minutes at 50ºC and 5 minutes at 95ºC and cDNA was diluted into 20µL of water, with 1-5µL used for further analysis.

Primer optimisation was carried out using PrimeScript III (Supplementary data, Tab 1) by comparing Cqs using combinations of forward and reverse primers at 0.3, 0.6 and 1µM and choosing the concentrations that recorded the lowest Cq. Probe optimisation was carried out by comparing Cqs obtained using 0.4µM or 0.8µM final probe concentration. Optimal annealing temperatures were determined by using SARS-CoV-2 cDNA and the temperature gradient option available on the BioRad CFX followed by melt curve analysis, together with SensiFast SYBR Green mix (Supplementary data, Tab 1) and optimal primer concentrations. Ideal annealing temperatures were identified as those resulting in the lowest Cq whilst retaining a single melt curve peak.

Minimum qPCR run times were established by preparing a single master mix, sufficient to carry out all experiments. The master mix consisted of SensiFast qPCR Probe mix, SARS-CoV-2 cDNA, and primers and probes specific for the targets and was kept on ice until required. 5µL aliquots were subjected to qPCR for decreasing denaturation and polymerisation times, with 1 second for each step being the minimum possible on the PCRMax and Techne instruments.

The experiments aimed at reducing RT times were initially carried out as using PCRBio One Step RT-qPCR reagent (Supplementary data, Tab 1), as the RT is supplied separately from the buffer. A 1x master mix of SARS-CoV-2 sample and EICAS RNA, CoV2-ID assay oligo blend (targeting Nsp10, N-gene, *JUN* and EICAS2) and RT-qPCR buffer was prepared and kept on ice. Immediately prior to each run, 10µL of that master mix was placed in a microfuge tube, 1µL of PCRBio RT was added and 2x5µL were added to two wells of a 48 well qPCR plate. The plate was briefly spun and subjected to different RT times, with qPCR times kept constant. All experiments were repeated using PrimeScript III (Supplementary data, Tab 1), but since this reagent is a single tube mixture of buffer and RT, a premix of RNAs, CoV2-ID and water was prepared, and 2x PrimeScript III mix was added just prior to each run.

RT-qPCR reactions were carried out on the following instruments: CFX (BioRad; Supplementary data, Tab 1), Eco (PCRBio; Supplementary data, Tab 1), Prime Pro (Techne; Supplementary data, Tab 1) or Mic (BMS; Supplementary data, Tab 1). Data were analysed using instrument software, Microsoft Excel for Mac v.16.38 and PRISM for Mac v.9.

Droplet digital PCR (ddPCR) reactions were set up as instructed in the operating guide using the QX200 droplet generator (BioRad), clear well semi-skirted 96 well plates, foil and PX1 PCR plate sealer (BioRad). Each 20µL reaction contained concentrations of cDNA corresponding to the ones used in parallel qPCR experiments, with the optimal primer and probe concentrations established for qPCR runs, which are slightly different from the recommended ones for primers (0.9µM) and probe (0.25µM). PCR reactions were carried out in 40µL volumes on a C1000 Touch Thermal cycler (BioRad) using the standard program of 10 minute enzyme activation at 95ºC, and 40 cycles of 30 seconds denaturation at 94ºC and 1 minute annealing/polymerisation at 60ºC, with the ramp rate set to 2ºC/second. The droplets were analysed immediately on the QX200 reader. RT-ddPCR reactions added a 1 hour reverse transcription at 45ºC at the start of the PCR protocol. Data were analysed using QuantaSoft Analysis Pro and QX Manager software (BioRad; Supplementary data, Tab 1).

Multiple cycle fluorescence detection PCR

Multiple cycle fluorescence detection PCR assays were carried out using SensiFast (Supplementary data, Tab 1) in 5µL volumes using the protocol shown in Table 2 on the CFX Connect instrument (BioRad). The first plate read after cycle 8 was used to establish a baseline fluorescence, thus allowing the calculation of fluorescence increases after cycles 20, 25, 30 and 35. In each case relative fluorescence increase was calculated by subtracting the cycle 8 fluorescence reading from the fluorescence readings after the respective cycles.

Results

Assay Design and characteristics

In silico analysis by PrimerBlast and BLAST analyses of primers, probes and amplicons signified that all virus oligonucleotide sequences are specific for SARS-CoV-2 and that the assays are not complementary

to any other coronavirus. Since the oligonucleotide manufacturer enclosed a cautionary note with primer and probe shipments indicating that they "could contain trace amounts of long oligo templates" specifying SARS-CoV-2 sequences, all panels were immediately assessed in qPCR assays without addition of template. None resulted in amplification signals, demonstrating that they were not contaminated with either SARS-CoV-2 or JUN templates. Assay details, oligonucleotide sequences, fluorophores, final optimised reaction conditions and PCR efficiencies are shown in Table 1. The supplementary data file contains the detailed optimisation results for primer and probe concentrations (Tab 2) and annealing temperatures (Ta) (Tab 3). All six assays resulted in efficient RT-qPCR assays, ranging from 94% to 103% (Table 1) with melt curves resulting in a single peak, indicating the amplification of a single amplicon (Supplementary Figure S1.

A conservative limit of quantification was established based on results from ddPCR experiments using Nsp10. Results from a five-fold serial dilution series indicated that quantification was linear to down to around 50 copies (Supplementary Figure S2a, b). In order to determine whether this was the approximate threshold of reliable and reproducible quantification, seven individual dilutions of the template were subjected to ddPCR assay. The results establish that this assay can reliably quantify 41±12 copies of viral target (Supplementary Figure S2c,d), although this limit is lower if additional probes are used (see below). In order to translate this to an RT-qPCR limit of detection (LOD) for viral targets, the sample containing 50 copies was diluted further to nominal 10, 5, 2 and 1 copies and subjected to qPCR amplification using the Nsp10 assay. This resulted in the detection of 5 copies by 12/12 replicates and two and one copies by 10/12 and 8/12 replicates, respectively (Figure 2a), with similar results obtained with Nsp12 (Figure 2b). A repeat experiment using the dilution that had a predicted two-copy per reaction detected Nsp10 presence in 24/24 reactions (Figure 2c). Underlying data are presented in supplementary data Tab 4.

Comparison of assay performance; individual or multiplex assays

To reduce sample processing time, reduce reagent usage and increase throughput it was desirable to optimise the assays to run in multiplex. Two viral targets (Nsp10 (FAM) and N-gene (Texas Red), *JUN* (Cy-5) and EICAS2 (HEX) panels were combined to form the initial assay. Cq values obtained from assays run individually were compared with those obtained in the multiplex reaction. The assays perform equally well in both conditions (Figure 3, supplementary data file Tab 5) with only JUN amplification being approximately two cycles later in the multiplex reaction. This was solved by increasing the JUN primer concentration to 1.3µM (supplementary data file Tab 5a).

The performance of the two EICAS assays and their effect on the amplification of the other markers was compared by carrying out four replicate multiplex RT-qPCR with either EICAS1 or EICAS2 as the internal control. Results were similar, suggesting that the inclusion of the additional primer set required for EICAS1 had no detectable adverse effect on assay performance (Supplementary data file Tab 6).

Assay validation

For validation of this test panel, 1µL RNA was used per sample to reanalyse all 28 clinical samples and our results were 100% concordant (Table 3; Cqs are shown in supplementary data file Tab 7). For sample A8, Broomfield Hospital recorded discordant ORF1ab/N-gene results but these were positive for both markers when tested with our panel. Six positive and four negative samples were also tested using a commercial diagnostic kit (Sansure), with comparable results. In this case, the commercial kit did not detect one of the viral targets (ORF1ab) in sample B1, which was detected both at Bromfield Hospital and with our panel. There was significant correlation between Cqs recorded for Nsp10 and N-gene (r (95%CI)=0.96 (0.89-0.98) as well as between Nsp 10 or N-gene and JUN (r=0.73 (0.45-0.88) and 0.86 (0.68-0.94, respectively (supplementary Figure S3 and supplementary data file, Tab 7). An analysis of all clinical samples using the D614G genotyping assay revealed that all isolates harboured the A to G transition, characteristic of the more infectious phenotype, whereas the control clinical sample and Twist BioScience control 1 were both wild type, G, at this location (supplementary data file, Tab 7)

Inclusion of the EICAS template in the assay panel permits some analysis of the quality of RNA extracted from patient samples. If inhibitors of the RT or the PCR are present in the clinical samples, an increase in Cq is expected for the EICAS assay compared with no template control samples, analogous to the principle underlying the SPUD assay (19). An analysis of the 28 samples revealed little, if any inhibition, with a median Cq of 27.07 (range 25.57-29.12) compared with the median Cq of 27.08 (range 27.54-26.91) recorded by no clinical template control samples (supplementary data file, Tab 7a).

The C to T transition at the -9 position in the Nsp10 F primer binding site of isolate MT412262 does not impede the binding of the CoV2-ID F primer to mutant target (Supplementary Figures S4a). The reverse is also true, in that the mutant primer binds efficiently to the WT target (Supplementary Figures S4b). In each case the qPCR data are in broad agreement with the ddPCR results. Targets with mutations at positions -10 and -7 at the N-gene primer binding site are also efficiently amplified by the CoV2-ID F primer (Supplementary Figures S5c), as is the WT sequence by the two mutant primers (Supplementary Figures S5d). Since a mutation has been identified for three isolates (MT506889/506904/506907) at position 2 of the 5'-end of the N-gene probe, the effect of that mutation on the efficiency of amplicon detection by the N-gene probe was investigated. Two specific probes were synthesised, one with (MuN) and one without (N-Pr2) the mutation at position 2 of the probe. Both gave virtually the same results (Supplementary Figure S5a), as did an alternative probe with WT sequences (Supplementary Figure S5b). The performance of both CoV2-ID and mutant primers with their respective templates was further analysed using an annealing temperature gradient analysis, which shows that the mutations have little effect on assay performance below 65ºC. Details of all underlying data for both qPCR and ddPCR results are listed in the supplementary data file Tabs 8, 8a, 8b and8c.

Conversion to a fiveplex assay and simplification

ddPCR data suggest that targeting two viral targets (Nsp10 and 12) using the same flurophore (FAM) increases the sensitivity of the assay by around 80% (Supplementary Figure S6a,b) and that there could be some benefit in a qPCR setting, especially with regards to further reducing the likelihood of a false

negative result (Supplementary Figure S6c,d with well statistics and Cqs listed in supplementary data file Tab 9).

To test this concept, Nsp12 was added as a third viral target to the fourplex CoV2-ID assay, making it a fiveplex, with two of the viral targets being detected on one channel. The results show that the assays work equally well (Supplementary Figure S7, with underlying data in supplementary data file Tab 10). Performance of the four- and fiveplex assays was further assessed in four additional patient samples and the results indicate that they perform comparably, with the viral targets being detected earlier in the fiveplex assay (Supplementary Figure S8, with underlying data in supplementary data file Tab 11). Finally, in order to determine whether the sensitivity of the assay could be increased further, the fiveplex assay was modified so that all three viral targets (Nsp10, Nsp12 and N-gene) were detected with FAM-labelled probes. Both qPCR (Figure S9a,b) and ddPCR (Figure S9c,d) data reveal that there is indeed a further increase in sensitivity (data in supplementary data file Tab 12).

Development of Rapid Cycling Conditions

In order to further improve the potential throughput of the assay in a diagnostic setting, the ability of the assay to perform adequately under short RT times and fast PCR conditions was tested. Data equivalent to the initial conditions of 10 mins RT, 5 seconds denaturation and 10 seconds polymerisation were obtained for all three viral targets, when the RT was reduced to 5 minutes and both denaturation and polymerisation times were 1 second, although in practice, the annealing/polymerisation step takes around 6 seconds, as the fluorescence scanning takes around five seconds. This resulted in a reduction in run times from 33 minutes 40 seconds to 20 minutes (Figure 4a, with data in supplementary data file Tab 13). The initial 5 second/10 second and final 1 second/1second conditions were applied to replicate fiveplex assays, and the results confirmed that all panels can be run using this protocol (Figure 4b; with data in supplementary data file Tab 13b).

The next aim was to try and reduce run times by further reducing the RT times. The results shown in supplementary Figure S10 (underlying Cqs are in supplementary data file, Tab 14) suggest that a 1-minute RT step results in Cqs similar to the 5-minute RT reaction, reducing run times to 16 minutes.

Reductions in run times can be achieved on instruments not designed to run as fast as the PCRMax/Techne, as shown for the BioRad CFX. Here the reduction in RT time from 10 minutes to 1 minute and cycling times from 95ºC/5 seconds and 60ºC/20 seconds, to 1 minute RT and 1 second each at 95ºC and 60ºC reduced the run time from 58 minutes to 32 minutes. The Cqs from seven targets present at a wide range of concentrations were compared and there was very little difference. Indeed, most of the targets recorded slightly lower Cqs with the fast run (supplementary data file, Tab 14a).

Since the cooling step is the slowest part of the PCR cycle in block-based qPCR instruments, reducing the temperature gap between denaturation and annealing/polymerisation temperatures should further reduce run times. Following an initial calibration run with a 1 minute RT step followed by 1 second 95ºC denaturation and 60ºC annealing/polymerisation steps, denaturation temperatures were reduced and

annealing/polymerisation temperatures were increased. Even without further modifications to primer or enzyme concentrations, the small differences in Cq (Figure 5, with Cqs in supplementary data file, Tab 15) indicate that this would be a potential method to reduce reaction times, in this case from 16 minutes to 14 minutes 11 seconds.

Multiple cycle fluorescence detection

We have developed a multiple cycle fluorescence detection (MCFD) protocol linked to a 5-level rating algorithm. This results in faster run times and permits the inclusion of the quantitative information inherent in real-time PCR without the confusion surrounding the use of quantification cycles. The feasibility of using this method rather than real-time detection was tested by comparing the performance of the two approaches using the same master mixes. Whereas the standard qPCR run took 43 minutes to complete, the MCFD run took just over 22 minutes. The results for five different concentrations of viral target, together with the NTC control are shown in Figure 6a, with the proposed algorithm in Figure 6b. All underlying MCFD data are shown in supplementary data file Tab 16.

Quantification potential

The inclusion of ddPCR quantified, internal EICAS, facilitates an indirect measurement of copy number, thus allows this RNA to function both as a measure of quality control, as well as an assessment of viral load.

The same quantity of Nsp10 target was detected using qPCR as well as digital PCR. The results shown in supplementary Figure S11a demonstrate how the reported Cq depends on the threshold setting, which is subjectively set by the operator or automatically determined by a software algorithm that can vary between runs and instruments. This interferes with accurate quantitative reporting of SARS-CoV-2 viral loads, as the highest and lowest threshold-dependent Cq recorded in that run varies by 8.7, ie corresponds to a 400-fold difference. In contrast, the copy numbers calculated using the ddPCR platform shows very little variation, recording an average copy number of 1163±61 (supplementary Figure S11b) Underlying data are shown in supplementary data file tab 17.

Discussion

The COVID19 pandemic, caused by the new SARS-CoV-2 virus, has led to the development of a wide range of diagnostic assays, many of which are RT-PCR based, utilise real time detection and report a Cq value to indicate presence or absence of the virus. It has become increasingly clear that there are significant inadequacies in the use and interpretation of many of these assays for testing and monitoring populations for viral spread. This has resulted in some confusion as to whether these diagnostic assays are capable of adequately addressing their three main functions: First, to identify patients presenting with symptoms consistent with COVID19 as SARS-CoV-2 positive or negative and, ideally, repeat testing to ensure that infected patients are free of virus before leaving isolation. Second, whilst an indication of viral load is useful to inform clinical, therapeutic decisions, the use of the subjective Cq is inappropriate

as it is not sufficiently reproducible or robust to allow an assessment of the validity of marginal results, i.e. those above cycles 35. Finally, widespread screening programmes of populations and environmental samples are required to monitor the spread of virus including mutations, given that a high percentage of those infected remain asymptomatic.

In general, the most critical features of a diagnostic assay are specificity and high sensitivity, with reliability, speed, and ease of use also being highly desirable. In addition, where large numbers of samples are processed cost saving on reagents is a serious consideration. Well-designed RT-qPCR assays certainly fulfil the first two criteria and have the potential to meet the remaining ones. Each of the three scenarios above requires a subtle variation on assay design and application. In the first case, the assay must be highly specific, reliable, sensitive and rapid. At this stage a binary positive or negative readout is sufficient. However, in the second scenario where therapy may be informed by an indication of viral load, the assay requires the same features with the addition of a quantitative assessment. Finally, widespread screening protocols benefit from low cost, high throughput and require simple binary readout without the absolute requirement to reduce time.

The assay described in this communication, termed CoV2-ID, has been developed to be adapted to any of the situations described.

The need for increased sensitivity and to minimise false negative results lead to the fiveplex CoV2-ID assay and demonstrates the importance of including more than a single viral target as part of a diagnostic kit. An RT-qPCR assay for SARS-CoV using two hydrolysis probes to increase sensitivity has been described a (21) and we have taken this one step further and have achieved ultimate sensitivity by detecting the three viral genes (Nsp10, Nsp12 and N) in one channel. This is a valid improvement because the diagnostic test does not need to distinguish between different viral targets, it just needs to detect the virus reliably. Compared with Nsp10 and Nsp12 alone, detection of three targets in one channel increases the sensitivity by around 3-fold in a qPCR assay and by 300% (Nsp10, Nsp12) and 100% (N) in a ddPCR assay.

While it may be desirable to measure viral load in patients exhibiting COVID19, there is considerable misunderstanding with regards to the quantitative interpretation of diagnostic RT-qPCR test results. These are routinely reported as Cqs, in the same way as those obtained from real-time quantitative (RT-qPCR) assays, where quantitative data are reported based on relative quantification, either against a reference gene or against a reference dilution curve (22). In either case, quantification depends on amplification efficiencies between target of interest and reference being similar. Furthermore, Cq values subject to inherent inter-run variation (23) and are operator, reagent- and instrument-dependent, with huge variations in Cq value ranges (up to 21 Cqs, the equivalent of a $2x10^6$-fold difference) reported for the same clinical virology run controls run in different laboratories (24). Consequently, results are not readily comparable when carried out using different master mixes, instruments and analysis criteria and should not be used without appropriate calibration standards (17). Regrettably, assays reported to date, for detection of detect SARS-CoV-2 do not include such reference materials, calibrated or just even quantified, and do not

use standard curves. Since Cq values are affected by numerous parameters, not least by operator intervention with regards to threshold settings, they must not be used quantitatively and should not be used to determine viral loads. Hence, in the absence of certified controls, the inclusion of an RNA control template, quantified by ddPCR, allows not just monitoring of the RT-qPCR reaction but also quantification of viral load. It must be stressed, however, that any quantitative data will still be laboratory-specific, and that use of the EICAS must be validated separately and repeatedly in different laboratories.

The EICAS serves additional control functions in the assay. Firstly it provides an indication of potential contaminants within the sample that may lead to inhibition of the RT or PCR, resulting in false negatives or reduced estimates of viral load. In addition, it has the potential to be included into samples and serve as an extraction control. Finally, the addition of an intronless human gene control permits screening of samples for nucleic acid content regardless of whether DNase is used during sample preparation.

The single tube reaction format, with low volumes and all reagents premixed, results in a simple workflow and the protocol has been modified to reduce the time taken to complete the assay. We have shown previously that the qPCR reactions times can be significantly reduced by decreasing the denaturation and polymerisation times and altering the denaturation and polymerisation temperatures (20). In this communication we have reduced both the RT and qPCR times, and so generated a test that can be run in around 15 minutes (on a suitable instrument). As there are applications where the aim of the test would be to detect the presence or absence of viral targets as quickly as possible, under these circumstances there is no requirement to run a complete real-time assay. Instead, measuring fluorescence towards the beginning of the run and then again at defined intervals throughout should detect any target-dependent amplification, whilst at the same time saving the considerable time it takes to scan a plate at the end of each cycle. Data are presented that demonstrate that this is indeed the case, and that fast run times can be achieved, even on an instrument such as the BioRad CFX, which is not optimised for maximum speed. On a fast instrument. e.g. those from PCRMax/Techne, run times can be reduced to as little as eight minutes, which is significantly faster than any other methodology, e.g. isothermal amplification, can achieve and so lends itself to incorporation into a point-of-care device. The use of defined fluorescence detection points also has the advantage of allowing the quantitative aspect of real-time PCR to be used to generate a viral load determination, without resorting to the use of a subjective Cq or controversial cut-off point. We propose detecting the first appearance of fluorescence over background and then monitoring its increase over a number of different cycles. This information can then be used to develop an algorithm that associates the first increase in fluorescence with a 5-level ratings system that can be used to inform further action. Importantly, any patient testing at level 1 should be retested immediately. Importantly, our protocol can be used with most conventional qPCR instruments, in contrast to a recent report that requires a specialist PCR instrument (25).

It is now widely accepted that SARS-CoV-2 mutations are arising constantly, although there is still no evidence for the evolution of distinct phenotypes in SARS-CoV-2 (26). Nonetheless, a SARS-CoV-2 variant carrying the Spike protein amino acid change D614G has replaced the original D614 variant (27), even where it was well established and has now become the most prevalent form in the global pandemic (28,

29). This mutation increases infectivity (30, 31) and may increase the severity in infected individuals (32), although it remains unclear what the impact of the mutation on transmission, disease, and vaccine and therapeutic development is (33). These data certainly support the finding that this variant is ubiquitous, as all of the UK isolates tested back as early as 14th April carry the D614G mutation. Unfortunately, we have not been able to obtain clinical samples preceding that date to determine whether the original strain ever circulated here in Essex.

Although human coronaviruses harbour a proofreading exoribonuclease, a number of location-specific mutations have been identified in the genome of SARS-CoV-2 that result in potential mismatches with all published primer and probe sequences (https://covid19.edgebioinformatics.org/#/assayValidation) (15). Hence, it is important for any assay to maintain routine verification of sequence mutations in primer and, to a lesser degree, probe binding region of the viral genome, as recommended by the American Society for Microbiology COVID-19 International Summit (34). CoV2-ID targets three viral genes, as this allows scope for the test to remain accurate even if mutations arise at the 3'-ends of the primers that could result in false-negative results.

However, in order to establish just what the consequences of mutations are, we have analysed the effects of mutations identified in the forward primers of two of the panels as well as in one of the probes. Primer BLAST analysis of the Nsp10 primers identified a variant (MT412262) with a C to T transition at position -9 of the F primer. There was also no difference in sensitivity when the mutant primer was used to amplify the reference strain RNA. BLAST search identified a C to T transition at position -10 in the N gene F primer binding site in a number of isolates (MT607612/481905/496997/467255/467251), which according to a recent paper has a frequency 0.006% (35). That publication also identifies a transversion, from A to T at position -7 (frequency 0.006%), which is not detected with BLAST. Neither of these mutations affected the accuracy of the N-gene assay, as the Cqs recorded by all three primers are essentially the same. BLAST searches also identified two mutations at the N-gene probe binding site, one a G to T transversion at 5'-end nucleotide 3 (MT520257/459840) the other a C to T transition at nucleotide 5 (MT506889/506904/506907). Their respective frequencies are 0.053% and 0.029%, respectively. There was no discernible effect on the ability of the mutated probe to detect the wild-type sequences on either reference sequence.

CoV2-ID is presented as an adaptable assay that can be applied to all SARS-CoV-2 detection and quantification applications. In presenting the development of this assay we also sought to provide maximum transparency for the verification process, effect of protocol variations and the requirement for adequate standards and controls in order for the assay to be reliable and robust. The current pandemic has revealed shortcomings in global response procedures and it is essential, that public health institutes, regulatory bodies and standards organisations to adopt a shared set of guidelines, protocols and standards that allow a common and meaningful interpretation of any emerging molecular testing regimen.

In conclusion, we have used the MIQE guidelines to design, develop, optimise and validate CoV2-ID, an enhanced, value-added RT-qPCR assay specific for SARS-CoV-2. It is robust, sensitive and is optimised for a rapid protocol, providing the opportunity for high throughput, multiplex viral detection with the potential to quantify viral load. Its design minimises the likelihood of assay failure causing false negative test results and its robustness provides a promise for its further development as an extreme PCR assay for use with point of care devices.

Declarations

This study was approved by the Research Ethics panel of the University's Faculty for Health, Education, Medicine and Social Care, reference HEMS-FREP 19/20/039. Analyses were performed on existing and anonymised RNA samples collected during standard diagnostic tests, with no clinical or epidemiological data available, apart from the reported Cqs. Consent was not required as the Human Tissue Authority has indicated that stored samples that have been taken for diagnosis and remain after the diagnostic procedure has been completed can be used in approved research, providing that all samples are anonymised to researchers.

Author contributions

Stephen Bustin initiated this project, designed all assays, carried out all the laboratory work, co-analysed the data and co-drafted the manuscript.

Amy Coward extracted all RNA samples and ran the RT-qPCR assays in the Microbiology laboratory at Broomfield Hospital. She contributed to the drafting of this manuscript.

Garry Sadler carried out the quality controls on patient samples, set up the hospital’s qPCR instrument, evaluated and selected all their reagents. He contributed to the drafting of this manuscript.

Louise Teare was the clinical lead and supervised patient selection, evaluated Broomfield’s results and helped draft this manuscript.

Tania Nolan assisted with assay design, co-analysed the data and co-drafted this manuscript.

Competing Interests

None of the authors have any competing interest to declare.

References

1. Wu F, Zhao S, Yu B et al. A new coronavirus associated with human respiratory disease in China. Nature. 2020;579:265-269.
2. Zhou P, Yang XL, Wang XG et al. A pneumonia outbreak associated with a new coronavirus of probable bat origin. Nature. 2020;579:270-273.

3. Shyu D, Dorroh J, Holtmeyer C et al. Laboratory Tests for COVID-19: A Review of Peer-Reviewed Publications and Implications for Clinical Ulse. Mo Med. 2020;117:184-195.
4. Li C, Ren L. Recent progress on the diagnosis of 2019 Novel Coronavirus. Transbound Emerg Dis. 2020;67:1485-1491.
5. Lalli MA, Chen X, Langmade SJ et al. Rapid and extraction-free detection of SARS-CoV-2 from saliva with colorimetric LAMP. medRxiv. 2020
6. Park GS, Ku K, Baek SH et al. Development of Reverse Transcription Loop-Mediated Isothermal Amplification Assays Targeting Severe Acute Respiratory Syndrome Coronavirus 2 (SARS-CoV-2). J Mol Diagn. 2020;22:729-735.
7. Dara M, Talebzadeh M. CRISPR/Cas as a Potential Diagnosis Technique for COVID-19. Avicenna J Med Biotechnol. 2020;12:201-202.
8. Xiang X, Qian K, Zhang Z et al. CRISPR-cas systems based molecular diagnostic tool for infectious diseases and emerging 2019 novel coronavirus (COVID-19) pneumonia. J Drug Target. 20201-5.
9. Bustin SA, Nolan T. RT-qPCR Testing of SARS-CoV-2: A Primer. Int J Mol Sci. 2020;21:3004.
10. Vogels CBF, Brito AF, Wyllie AL et al. Analytical sensitivity and efficiency comparisons of SARS-CoV-2 RT-qPCR primer-probe sets. Nat Microbiol. 2020
11. Dharavath B, Yadav N, Desai S et al. A one-step, one-tube real-time RT-PCR based assay with an automated analysis for detection of SARS-CoV-2. Heliyon. 2020;6:e04405.
12. Shen M, Zhou Y, Ye J et al. Recent advances and perspectives of nucleic acid detection for coronavirus. J Pharm Anal. 2020
13. Kucirka LM, Lauer SA, Laeyendecker O, Boon D, Lessler J. Variation in False-Negative Rate of Reverse Transcriptase Polymerase Chain Reaction-Based SARS-CoV-2 Tests by Time Since Exposure. Ann Intern Med. 2020
14. Li Y, Yao L, Li J et al. Stability issues of RT-PCR testing of SARS-CoV-2 for hospitalized patients clinically diagnosed with COVID-19. J Med Virol. 2020;92:903-908.
15. Osório NS, Correia-Neves M. Implication of SARS-CoV-2 evolution in the sensitivity of RT-qPCR diagnostic assays.[letter]. Lancet Infect Dis 2020
16. Moses SE, Warren CR, P, Curtis JA,S Holme, J Jain, N Brookes, KJ, Hanley QS. Endpoint PCR Detection of Sars-CoV-2 RNA. medRxiv. 2020
17. Bustin SA, Benes V, Garson JA et al. The MIQE guidelines: minimum information for publication of quantitative real-time PCR experiments. Clin Chem. 2009;55:611-622.
18. World Health O. Laboratory Testing for Coronavirus Disease (COVID-19) in Suspected Human Cases: Interim Guidance, 19 March 2020, World Health Organization, Geneva. 2020
19. Nolan T, Hands RE, Ogunkolade W, Bustin SA. SPUD: a quantitative PCR assay for the detection of inhibitors in nucleic acid preparations. Anal Biochem. 2006;351:308-310.
20. Bustin SA. How to speed up the polymerase chain reaction. Biomol Detect Quantif. 2017;12:10-14.

21. Yip SP, To SS, Leung PH, Cheung TS, Cheng PK, Lim WW. Use of dual TaqMan probes to increase the sensitivity of 1-step quantitative reverse transcription-PCR: application to the detection of SARS coronavirus. Clin Chem. 2005;51:1885-1888.
22. Bustin SA. Absolute quantification of mRNA using real-time reverse transcription polymerase chain reaction assays. J Mol Endocrinol. 2000;25:169-193.
23. Hellemans J, Mortier G, De Paepe A, Speleman F, Vandesompele J. qBase relative quantification framework and software for management and automated analysis of real-time quantitative PCR data. Genome Biol. 2007;8:R19.
24. Fryer JF, Baylis SA, Gottlieb AL et al. Development of working reference materials for clinical virology. J Clin Virol. 2008;43:367-371.
25. Asghari E, Höving A, van Heijningen P et al. Ultra-fast one-step RT-PCR protocol for the detection of SARS-CoV-2. medRxiv. 2020
26. van Dorp L, Acman M, Richard D et al. Emergence of genomic diversity and recurrent mutations in SARS-CoV-2. Infect Genet Evol. 2020;83:104351.
27. Koyama T, Weeraratne D, Snowdon JL, Parida L. Emergence of Drift Variants That May Affect COVID-19 Vaccine Development and Antibody Treatment. Pathogens. 2020;9
28. Biswas NK, Majumder PP. Analysis of RNA sequences of 3636 SARS-CoV-2 collected from 55 countries reveals selective sweep of one virus type. Indian J Med Res. 2020;151:450-458.
29. Korber B, Fischer WM, Gnanakaran S et al. Tracking changes in SARS-CoV-2 Spike: evidence that D614G increases infectivity of the COVID-19 virus. Cell. 2020;182:1-16.
30. Zhang L, Jackson CB, Mou H et al. The D614G mutation in the SARS-CoV-2 spike protein reduces S1 shedding and increases infectivity. bioRxiv. 2020
31. Yurkovetskiy L, Pascal KE, Tompkins-Tinch C et al. SARS-CoV-2 Spike protein variant D614G increases infectivity and retains sensitivity to antibodies that target the receptor binding domain. bioRxiv. 2020
32. Eaaswarkhanth M, Al Madhoun A, Al-Mulla F. Could the D614G substitution in the SARS-CoV-2 spike (S) protein be associated with higher COVID-19 mortality. Int J Infect Dis. 2020;96:459-460.
33. Grubaugh ND, Hanage WP, Rasmussen AL. Making Sense of Mutation: What D614G Means for the COVID-19 Pandemic Remains Unclear. Cell. 2020
34. Report from the American Society for Microbiology COVID-19 International Summit, 23 March 2020: Value of Diagnostic Testing for SARS-CoV-2/COVID-19. [editorial]. mBio 2020;11(2)
35. Khan KA, Cheung P. Presence of mismatches between diagnostic PCR assays and coronavirus SARS-CoV-2 genome. Royal Society Open Science. 2020;7:200636.

Tables

Table 1. Details of oligonucleotide sequences, fluorophores, optimal concentrations and annealing temperatures used for the detection of SARS-CoV-2 targeting nsp10, N-gene, nsp12, JUN and EICAS,

collectively referred to as CoV2-ID. All oligonucleotides are listed in the 5'-3' direction. Nucleotides that differ from the SARS-CoV-2 reference sequence, but have been detected at low frequency are shown in red. Oligonucleotides are based on the following accession numbers: Reference SARS-CoV-2: NC_045512; mutant SARS-CoV-2: MT412262 (F-primer 10Mu); MT607612/481905/496997/ 467255/467251 (F-primers NA and NB); MT506889/506904/506907 (Probe MuN); c-JUN: NM_002228.4.

Target	Target	Amplicon	Oligonucleotides (5'-3')	Final conc	Ta	Assay efficiency
SARS-CoV-2	Nsp10	85 bp	F: GGATCAAGAATCCTTTGGTGG	1 µM	64.0°C	94%
			R: GTCACAAAATCCTTTAGGATTTGGA	1µM		
			Pr: FAM-CATCGTGTTGTCTGTACTGCCGTTGCC	0.4µM		
	N-gene	88 bp	F: GCTGCTAGACAGATTGAAC	1 µM	60.5°C	96%
			R: AGCAGATTTCTTAGTGACAGTTTG	1µM		
			Pr1:-TR-ATGTCTGGTAAAGGCCAACAACAACA	0.4µM		
			Pr2: TR/FAM-TCTGGTAAAGGCCAACAACAACAAGG	0.4µM		
	Nsp12	96 bp	F: CATCCCTACTATAACTCAAATGAA	1 µM	62.0°C	99%
			R: GTCATAGTACTACAGATAGAGACAC	1µM		
			Pr: FAM-TGCAAAGAATAGAGCTCGCACCGT	0.4µM		
	Mu-Nsp10	85 bp	(10Mu) GGATCAAGAATCTTTTGGTGG	1 µM	61.0°C	
	Mu-N-gene	88 bp	(NA) GCTGCTTGACAGTTTGAAC	1 µM	62.0°C	
			(NB) GCTGCTTGATAGATTGAAC	1µM	60.3°C	
			MuN: TR-TTTGGTAAAGGCCAACAACAACAAGG	0.4µM		
	D614G mutation	104 bp	F: CACCAGGAACAAATACTTC	1 µM		
			R: CCAAGTAGGAGTAAGTTGA	1µM		
			WT: FAM-ctttAtcAggAtgTtaact	0.4µM		
			Mu: HEX-ctttAtcAggGtgTtaact	0.4µM		
mRNA control	*JUN*	88 bp	F: CGCCTGATAATCCAGTCCA	1.3 µM	60.5°C	103%
			R: GCTCATCTGTCACGTTCTTG	1.3µM		
			Pr:- Cy5-CACATCACCACCACGCCGACC	0.4µM		
EICAS1	-	58 bp	F: AACAACCACACCAAAAC	1 µM	60.7°C	98%
			R: GGAGGTTTTAGTTTGG	1µM		
			Pr: HEX-CACACAACACCAACAAAACCAAACA	0.4µM		
	rArArCrArArCrCrArCrArCrCrArArArArCrCrArCrArCrArArCrArCrCrArArCrArArArArCrCrArArArCrArCrCrA rArArCrUrArArArArCrCrUrCrC					
EICAS2	-	65 bp	Pr: HEX-CACACAACACCAACAAAACCAAACA	0.4µM		96%
	rCrGrCrCrUrGrArUrArArUrCrCrArGrUrCrCrArUrCrArCrArCrArArCrArCrCrArArCrArArArArCrCrArArArCr ArCrArArGrArArCrGrUrGrArCrArGrArUrGrArGrC					

Table 2. Protocol for multiple cycle fluorescence detection.

Step	Reaction	Temperature (ºC)	Time (sec)	Number of cycles
	Activation	95	30	-
Amplification 1	Denaturation	93	1	7
	Polymerisation	64	1	
Detection cycle 8	Denaturation	93	1	1
	Polymerisation	64	1	
Amplification 2	Denaturation	93	1	6
	Polymerisation	64	1	
Detection 15	Denaturation	93	1	1
	Polymerisation	64	1	
Amplification 3	Denaturation	93	1	4
	Polymerisation	64	1	
Detection cycle 20	Denaturation	93	1	1
	Polymerisation	64	1	
Amplification 4	Denaturation	93	1	4
	Polymerisation	64	1	
Detection cycle 25	Denaturation	93	1	1
	Polymerisation	64	1	
Amplification 5	Denaturation	93	1	4
	Polymerisation	64	1	
Detection cycle 30	Denaturation	93	1	1
	Polymerisation	64	1	
Amplification 6	Denaturation	93	1	4
	Polymerisation	64	1	
Detection cycle 35	Denaturation	93	1	1
	Polymerisation	64	1	

Table 3. Validation of 28 RNAs extracted from patients attending Broomfield Hospital between April and June 2020. The four positive (A-D) and single negative batches were collected at different times. Negative test results are highlighted in green. The Viasure data were obtained at the hospital, and ten of the samples were screened using a commercial kit (Sansure). The result of the genotyping tests are also shown.

		Viasure			COV2-ID				Sansure			
Sample	Date	ORF1ab	N	IC	Nsp10	N	JUN	EICAS	ORF1ab	N	IC	D614G status
A1	24/04/2020	+ve	+ve	+ve	+ve	+ve	+ve	+ve	-	-	-	Mutant (G)
A2	29/04/2020	+ve	+ve	+ve	+ve	+ve	+ve	+ve	-	-	-	Mutant (G)
A3	30/04/2020	+ve	+ve	+ve	+ve	+ve	+ve	+ve	-	-	-	Mutant (G)
A4	01/05/2020	+ve	+ve	+ve	+ve	+ve	+ve	+ve	+ve	+ve	+ve	Mutant (G)
A5	01/05/2020	+ve	+ve	+ve	+ve	+ve	+ve	+ve	-	-	-	Mutant (G)
A6	03/05/2020	+ve	+ve	+ve	+ve	+ve	+ve	+ve	-	-	-	Mutant (G)
A7	03/05/2020	+ve	+ve	+ve	+ve	+ve	+ve	+ve	-	-	-	Mutant (G)
A8	03/05/2020	-ve	+ve	+ve	+ve	+ve	+ve	+ve	-	-	-	Mutant (G)
B1	14/04/2020	+ve	+ve	+ve	+ve	+ve	+ve	+ve	-ve	+ve	+ve	Mutant (G)
B2	26/04/2020	+ve	+ve	+ve	+ve	+ve	+ve	+ve	+ve	+ve	+ve	Mutant (G)
B3	26/04/2020	+ve	+ve	+ve	+ve	+ve	+ve	+ve	+ve	+ve	+ve	Mutant (G)
B4	26/04/2020	+ve	+ve	+ve	+ve	+ve	+ve	+ve	+ve	+ve	+ve	Mutant (G)
B5	27/04/2020	+ve	+ve	+ve	+ve	+ve	+ve	+ve	+ve	+ve	+ve	Mutant (G)
C1	14/04/2020	+ve	+ve	+ve	+ve	+ve	+ve	+ve	-	-	-	Mutant (G)
C2	15/04/2020	+ve	+ve	+ve	+ve	+ve	+ve	+ve	-	-	-	Mutant (G)
C3	15/04/2020	+ve	+ve	+ve	+ve	+ve	+ve	+ve	-	-	-	Mutant (G)
C4	15/04/2020	+ve	+ve	+ve	+ve	+ve	+ve	+ve	-	-	-	Mutant (G)
C5	17/04/2020	+ve	+ve	+ve	+ve	+ve	+ve	+ve	-	-	-	Mutant (G)
C6	17/04/2020	+ve	+ve	+ve	+ve	+ve	+ve	+ve	-	-	-	Mutant (G)
C7	19/04/2020	+ve	+ve	+ve	+ve	+ve	+ve	+ve	-	-	-	Mutant (G)
D1	13/06/2020	+ve	+ve	+ve	+ve	+ve	+ve	+ve	-	-	-	Mutant (G)
D2	27/04/2020	+ve	+ve	+ve	+ve	+ve	+ve	+ve	-	-	-	Mutant (G)
D3	13/06/2020	+ve	+ve	+ve	+ve	+ve	+ve	+ve	-	-	-	Mutant (G)
E1	N/A	-ve	-ve	+ve	-ve	-ve	+ve	+ve	-ve	-ve	+ve	N/A
E2	N/A	-ve	-ve	+ve	-ve	-ve	+ve	+ve	-ve	-ve	+ve	N/A
E3	N/A	-ve	-ve	+ve	-ve	-ve	+ve	+ve	-	-	-	N/A
E4	N/A	-ve	-ve	+ve	-ve	-ve	+ve	+ve	-ve	-ve	+ve	N/A
E5	N/A	-ve	-ve	+ve	-ve	-ve	+ve	+ve	-ve	-ve	+ve	N/A
n=	28											

Figures

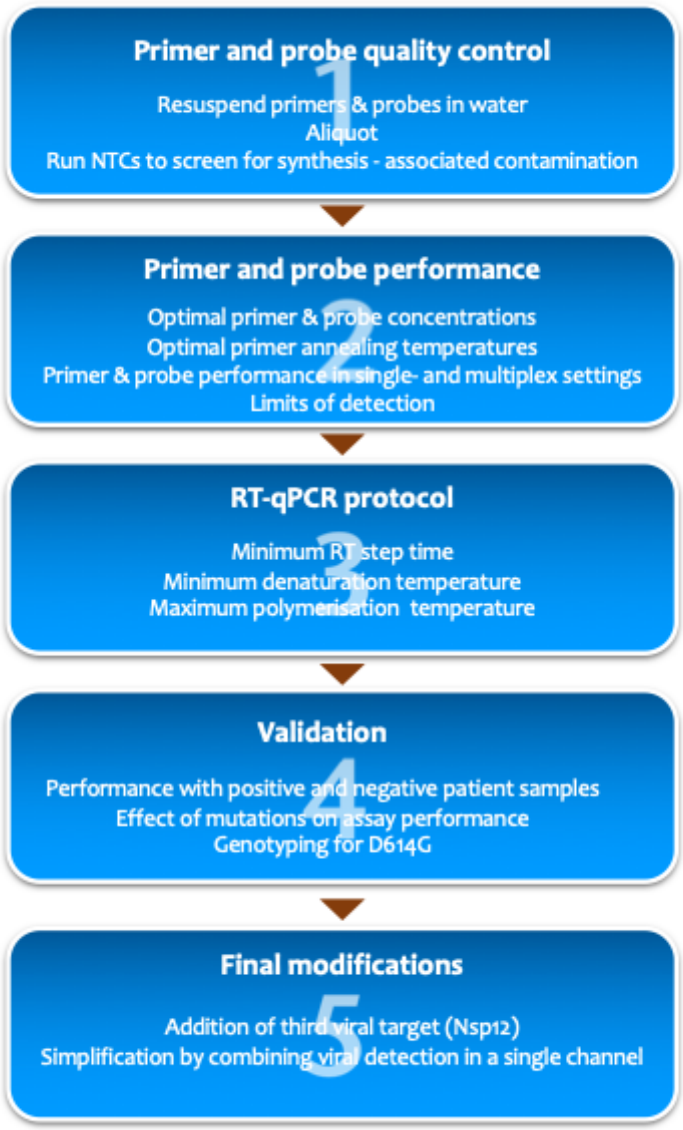

Figure 1

MIQE-compliant workflow used to characterise, optimise and validate the components that make up CoV2-ID assay.

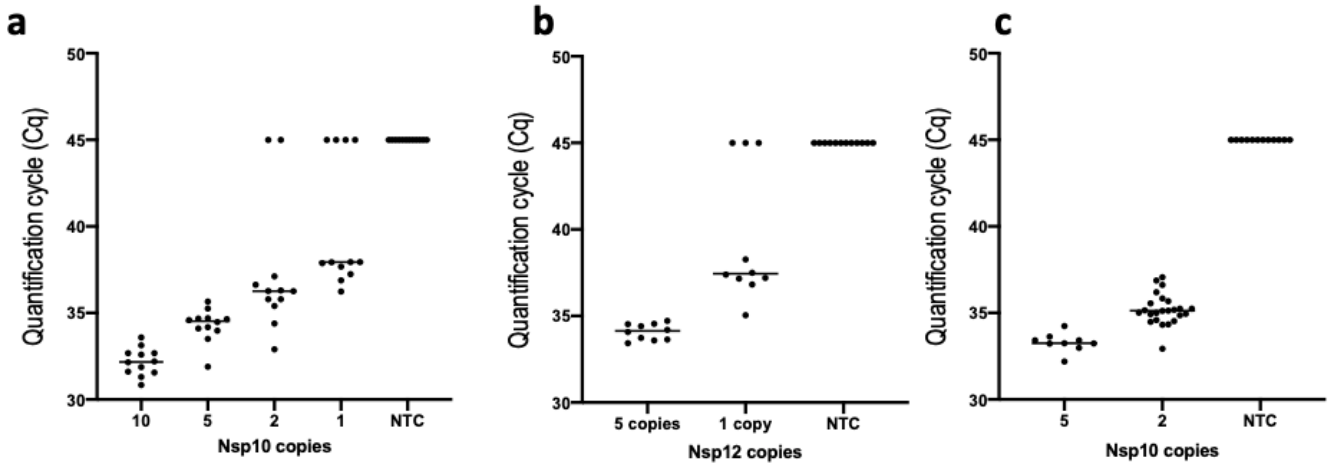

Figure 2

LOD for Nsp10 and 12. A. Individual Cqs from 12 replicates of patient-derived samples containing nominal SARS-CoV-2 copies of 10, 5, 2 and 1 (determined by ddPCR), detected using the Nsp10 assay. B. Cqs from 10 replicates with 5 or 1 copy of target obtained for Nsp12. C. Cqs from repeat reaction of 10 replicates with 5 or 1 copy of target obtained for Nsp10.

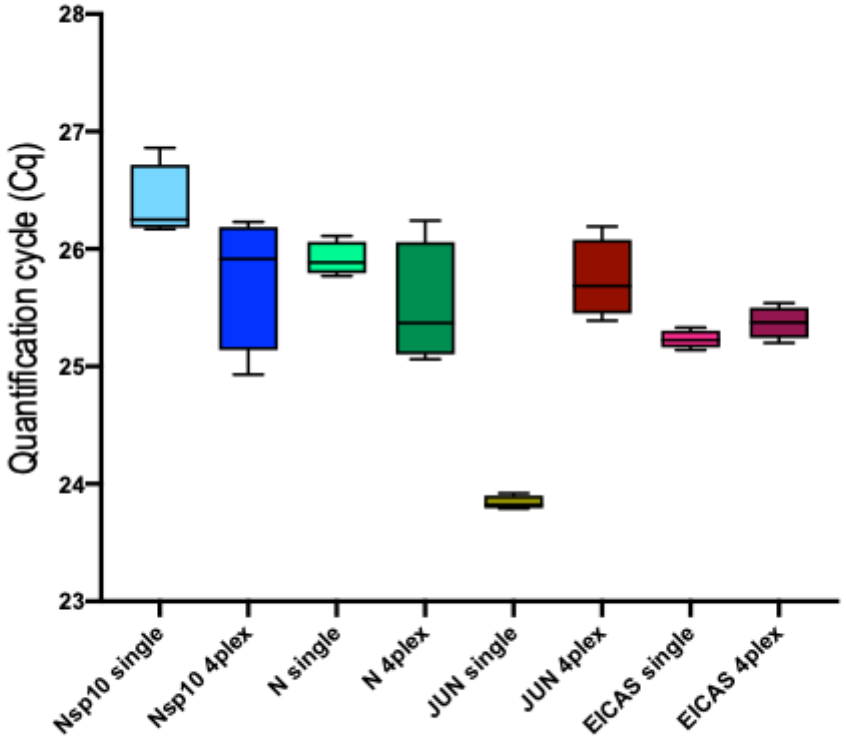

Figure 3

Comparison of Cqs obtained from single- and multiplex assays for the four panels making up CoV2-ID. The line through the box shows median Cqs and the whiskers denote minimum and maximum Cqs.

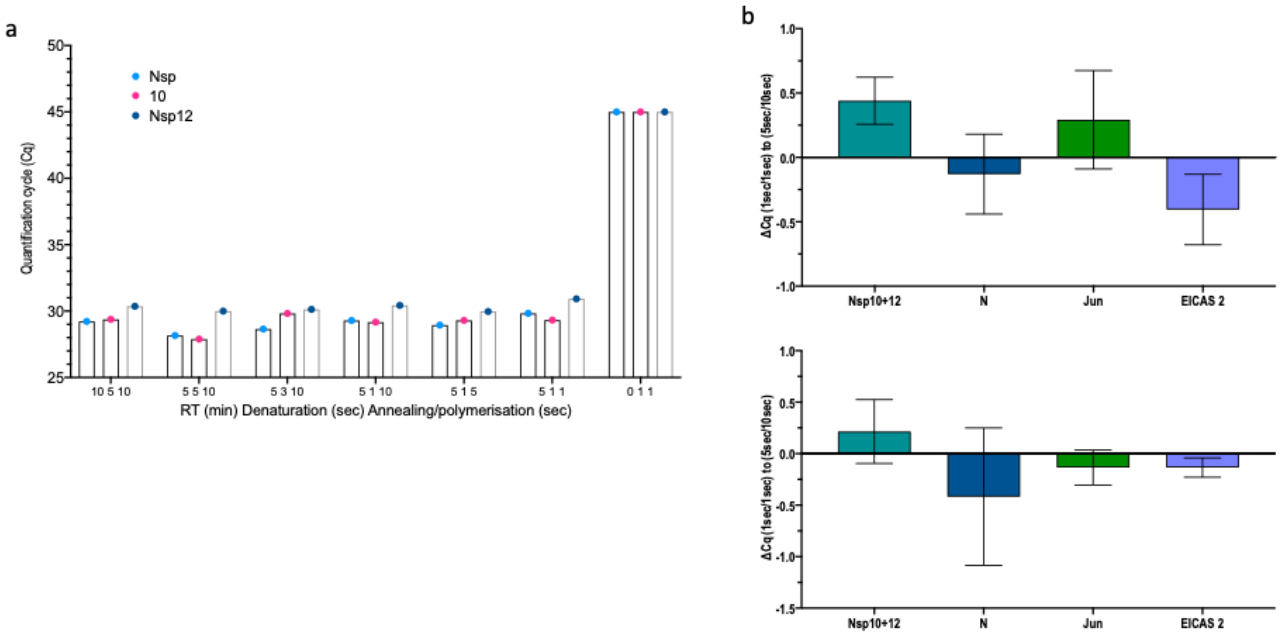

Figure 4

Reduction in qPCR times. A. Cqs obtained for Nsp10, 12 and N-gene by reduction of qPCR times from 5 second denaturation and 10 second annealing polymerisation to 1 second each. B. Comparison of the initial (5 seconds/10 seconds) and final (1 second/1second) denaturation/annealing and polymerisation qPCR protocols. The assays were run in duplicate, with the plots showing the ΔCqs between the longer and shorter timings.

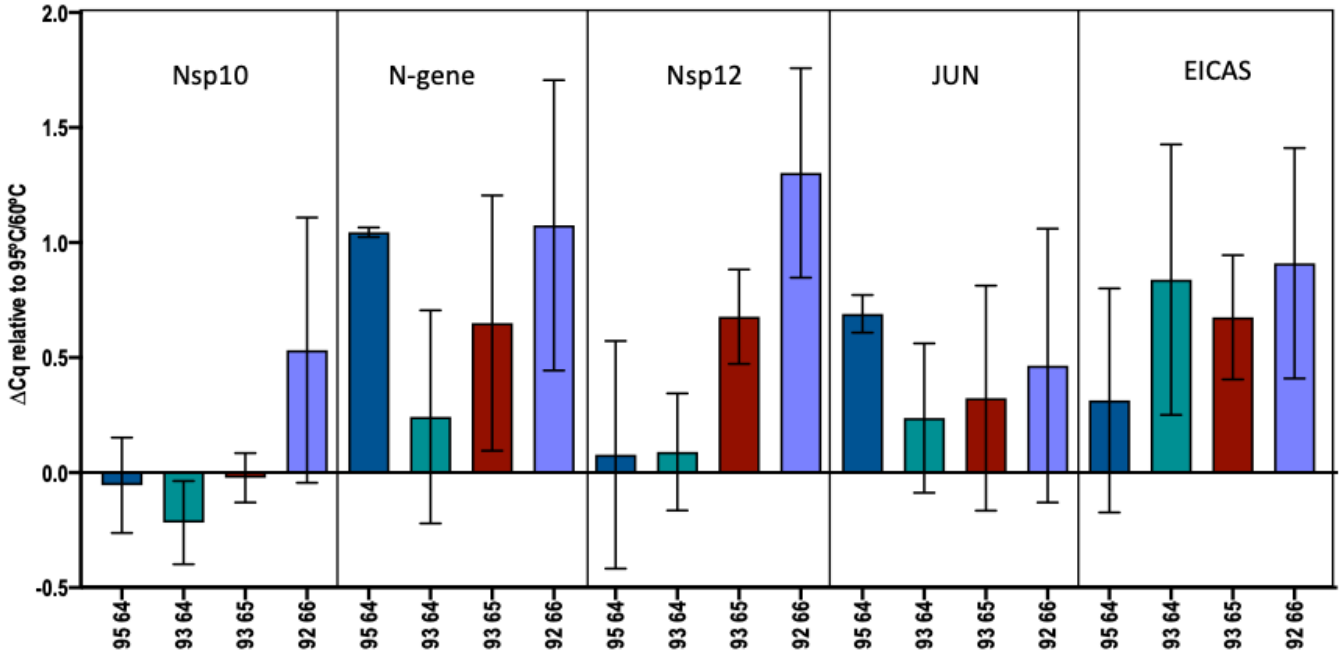

Figure 5

Reduction in denaturation and polymerisation times. The ΔCqs for each of the five targets are plotted for each of the different temperatures used to carry out the PCR reactions.

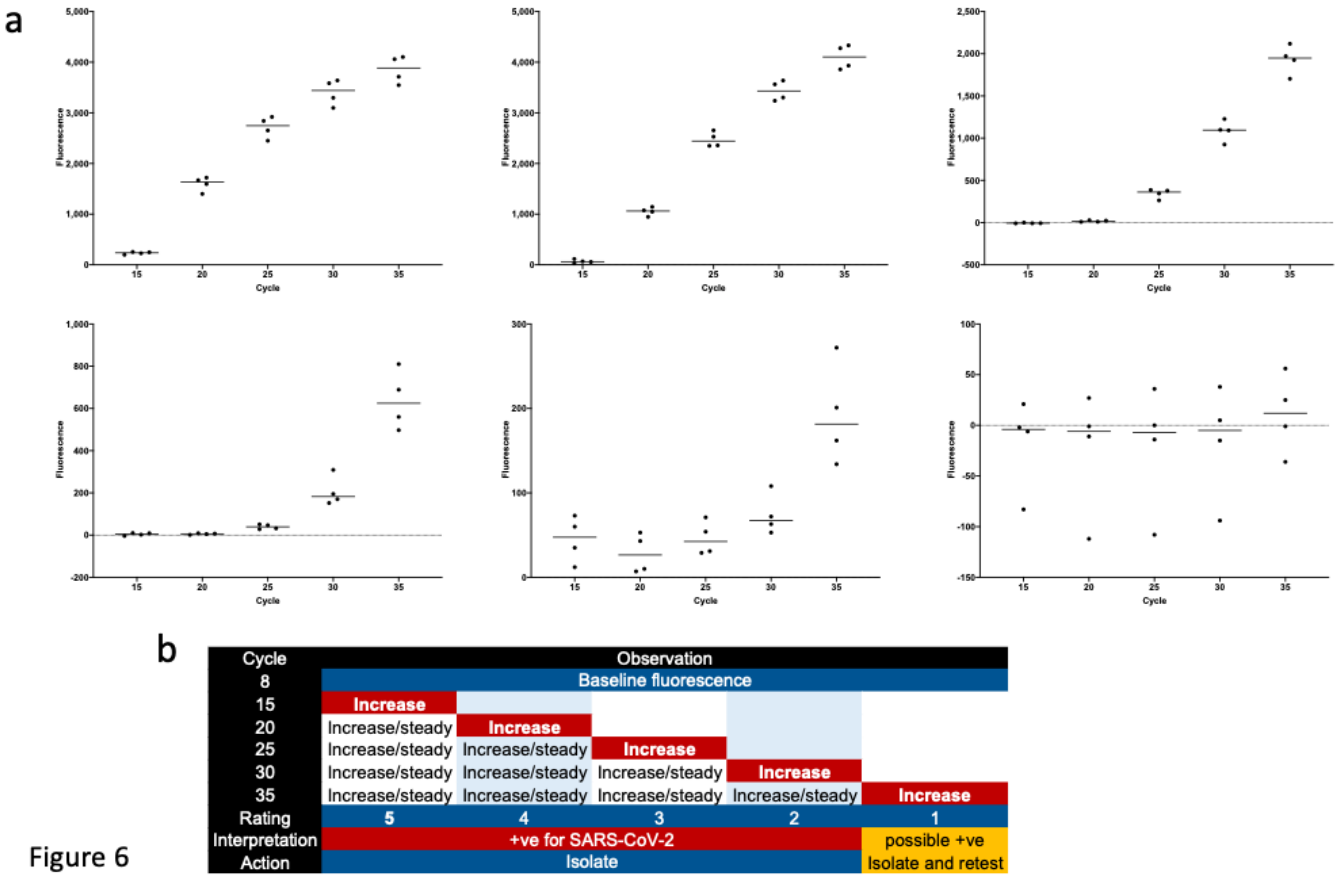

Figure 6

Figure 6

Multiple cycle fluorescence detection PCR results. A. Four replicates were assayed for five samples containing different concentrations of Nsp12 amplicons, together with a NTC. Fluorescence data were collected at cycles 8, 15, 20, 25, 30 and 35 and for each replicate the fluorescence recorded at cycle 5 was subtracted from the fluorescence recorded at each subsequent fluorescence collection cycle. The difference in fluorescence was plotted for each cycle, with the horizontal bar indicating the median fluorescence. The run took just over 22 minutes to complete. B. Algorithm incorporating the fluorescence data into a diagnostic assessment tool, obviating the need to deal with Cqs and cut-offs.

Supplementary Files

This is a list of supplementary files associated with this preprint. Click to download.

- Supplementallegends090920.docx
- SuppFigFINAL.pdf
- Supplementaryfile020920.xlsx